

University of Nebraska - Lincoln

DigitalCommons@University of Nebraska - Lincoln

---

David Sellmyer Publications

Research Papers in Physics and Astronomy

---

4-11-2005

## High-temperature ferromagnetism in pulsed-laser deposited epitaxial (Zn,Mn)O thin films: Effects of substrate temperature

Aswini K. Pradhan

*Center for Materials Research, Norfolk State University, apradhan@nsu.edu*

Kai Zhang

*Center for Materials Research, Norfolk State University, Virginia*

S. Mohanty

*Center for Materials Research, Norfolk State University, Virginia*

J.B. Dadson

*Center for Materials Research, Norfolk State University, Virginia*

D. Hunter

*Center for Materials Research, Norfolk State University, Virginia*

*See next page for additional authors*

Follow this and additional works at: <https://digitalcommons.unl.edu/physics Sellmyer>

 Part of the [Physics Commons](#)

---

Pradhan, Aswini K.; Zhang, Kai; Mohanty, S.; Dadson, J.B.; Hunter, D.; Zhang, Jun; Sellmyer, David J.; Roy, U.N.; Cui, Y.; Burger, A.; Mathews, S.; Joseph, B.; Sekhar, B.R.; and Roul, B.K., "High-temperature ferromagnetism in pulsed-laser deposited epitaxial (Zn,Mn)O thin films: Effects of substrate temperature" (2005). *David Sellmyer Publications*. 11.

<https://digitalcommons.unl.edu/physics Sellmyer/11>

This Article is brought to you for free and open access by the Research Papers in Physics and Astronomy at DigitalCommons@University of Nebraska - Lincoln. It has been accepted for inclusion in David Sellmyer Publications by an authorized administrator of DigitalCommons@University of Nebraska - Lincoln.

---

**Authors**

Aswini K. Pradhan, Kai Zhang, S. Mohanty, J.B. Dadson, D. Hunter, Jun Zhang, David J. Sellmyer, U.N. Roy, Y. Cui, A. Burger, S. Mathews, B. Joseph, B.R. Sekhar, and B.K. Roul

# High-temperature ferromagnetism in pulsed-laser deposited epitaxial (Zn,Mn)O thin films: Effects of substrate temperature

A. K. Pradhan,<sup>a)</sup> Kai Zhang, S. Mohanty, J. B. Dadson, and D. Hunter  
*Center for Materials Research, Norfolk State University, 700 Park Avenue, Norfolk, Virginia 23504*

Jun Zhang and D. J. Sellmyer  
*Department of Physics and Astronomy and Center for Materials Research and Analysis,  
 University of Nebraska, Lincoln, Nebraska 68588-0113*

U. N. Roy, Y. Cui, and A. Burger  
*Department of Physics, Fisk University, 1000, 17 Avenue North, Nashville, Tennessee 37208*

S. Mathews, B. Joseph, B. R. Sekhar, and B. K. Roul  
*Institute of Physics, Sachivalaya Marg, Bhubaneswar-751 005, Orissa, India*

(Received 7 September 2004; accepted 18 February 2005; published online 8 April 2005)

We report on the observation of remarkable room-temperature ferromagnetism in epitaxial (Zn,Mn)O films grown by a pulsed-laser deposition technique using high-density targets. The optimum growth conditions were demonstrated from x-ray measurements, microstructure, Rutherford backscattering, micro-Raman, and magnetic studies. Superior ferromagnetic properties were observed in (Zn,Mn)O films grown at a substrate temperature of 500 °C and with an oxygen partial pressure of 1 mTorr. Ferromagnetism becomes weaker with increasing substrate temperature due to the formation of isolated Mn clusters irrespective of higher crystalline quality of the film.

© 2005 American Institute of Physics. [DOI: 10.1063/1.1897827]

Diluted magnetic semiconductors (DMS) that involve charge and spin degrees of freedom in a single material are expected to play an important role for the fabrication of potential device applications in which both memory and logic operations could be seamlessly integrated on a single device. These materials exhibit many interesting magnetic, magneto-optic, magneto-electronic, and other properties. Following the recent discovery<sup>1,2</sup> of ferromagnetism in Ga<sub>1-x</sub>Mn<sub>x</sub>As, with a Curie temperature  $T_c \approx 100$  K in the  $x=0.03-0.07$  range, Mn-based III-V DMS received much attention. However, the low magnetic ordering temperature in GaMnAs restricts its spintronic applications at room temperature. Following the theoretical prediction<sup>3</sup> that transition metals, especially Mn, doped with GaN and ZnO could show large ferromagnetic Curie temperature, numerous studies have been carried out on (Zn,Mn)O and (Ga,Mn)N systems. The recent discovery of ferromagnetism<sup>4-6</sup> in (Ga,Mn)N, at temperatures much higher than room temperature, has fueled hopes that these materials can indeed have a profound technological impact. However, there remain controversies about the origin of ferromagnetic behavior in GaMnN due to very poor solubility ( $\sim 3$  mol %) of Mn into Ga sublattice. Because of higher thermal solubility of Mn into ZnO ( $\sim 10$  mol %), it becomes obvious that the next candidate for studying magnetism in DMS materials is (Zn,Mn)O.

There are several reports<sup>7-9</sup> where ferromagnetism in bulk, nanostructures and Mn ion-implanted ZnO films has been observed. The reported ferromagnetic transition temperature, however, varies from 50 to 300 K. On the other hand, ZnMnO films prepared by magnetron sputtering,<sup>10</sup> pulsed-laser deposition<sup>11</sup> (PLD), and polycrystalline samples<sup>12</sup> did not show ferromagnetic behavior. A recent

report<sup>13</sup> of ferromagnetism in both ZnMnO bulk and thin film with ferromagnetic Curie temperature  $T_c > 420$  K has aroused intense interest in this wide band gap semiconductor for possible spintronic applications. There are large controversies and difference in results, which are attributed to the different synthesis techniques and different degree of Mn clusters that are responsible for antiferromagnetic behavior. In this letter, we demonstrate the remarkable room-temperature ferromagnetism in epitaxial ZnMnO films grown by the PLD technique using high-density targets. We have elucidated the optimum substrate temperature for the observation of the ferromagnetism in this system from x-ray measurements, microstructure, Rutherford backscattering (RBS), micro-Raman, and magnetic studies.

ZnMnO/Sapphire(0001) epitaxial films were grown by the PLD technique (KrF excimer,  $\lambda=248$  nm, laser repetition rate of 5 Hz) with a pulse energy density of 1–2 J/cm<sup>2</sup> and utilizing both target and substrate rotation facilities. High-density Zn<sub>0.94</sub>Mn<sub>0.06</sub>O (ZnMnO) target was used. Stoichiometric amount of ZnO and MnO<sub>2</sub> (both 99.99% purity) powders were mixed, calcined at 400 °C for 12 h followed by isostatic pressing at 400 MPa, and finally sintered at 500 °C in order to make high-density target. The films were deposited with a substrate temperature  $T_s=500-650$  °C, keeping oxygen partial pressure  $PO_2=1$  mTorr. Clean single-crystalline sapphire substrates were loaded to the chamber and heated just after the ultimate base pressure  $<4 \times 10^{-8}$  Torr is reached. The x-ray diffraction (XRD) of the films was performed in a Rigaku x-ray diffractometer using Cu K $\alpha$  radiation. The Raman spectra were recorded using a LabRam micro-Raman spectrometer with He–Ne laser excitation (wavelength: 632.8 nm). The magnetization was measured using Quantum Design superconducting quantum interference device (MPMS).

<sup>a)</sup> Author to whom all correspondence should be addressed; electronic mail: apradhan@nsu.edu

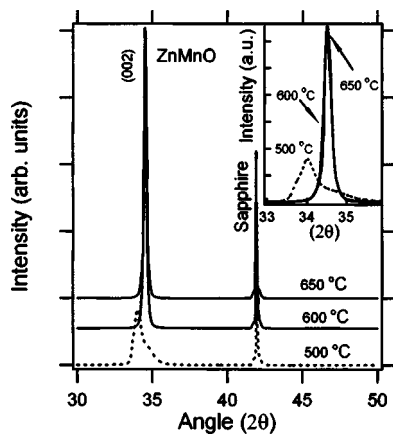


FIG. 1. XRD pattern of ZnMnO films grown on sapphire substrates at different substrate temperatures. The inset shows the rocking curves for (002) reflection of the film grown at different temperatures.

Figure 1 shows the XRD patterns of ZnMnO/sapphire (0001) films grown at three different  $T_s$  values with a constant  $PO_2$ . The XRD patterns for all films reveal only one strong orientation (002), illustrating the epitaxial nature of the film. The rocking curves for the epitaxial growth of the films with different substrate temperatures are shown in the inset of Fig. 1. The full-width half maxima (FWHM) calculated from x-ray (002) line broadening shows that FWHM decreases from  $0.4^\circ$  to  $0.17^\circ$  with increasing  $T_s$  from 500 to 650 °C at  $PO_2=1$  mTorr, illustrating the higher crystalline quality of the film grown at a higher temperature. It is interesting to note that not only the peak position of the film grown at 500 °C shifts to lower angle, but also it is poorer in crystalline quality although it is epitaxial. A peak shift to lower values indicates that Mn is incorporated into the Zn lattice which is consistent with the previous report.<sup>7</sup> However, the peak broadening observed for the film grown at 500 °C is mainly a consequence of poor crystalline quality most probably due to the presence of ZnMnO in ZnO.

The atomic force microscopy (AFM) images of as-grown ZnMnO films are shown in Figs. 2(a)–2(c). The re-

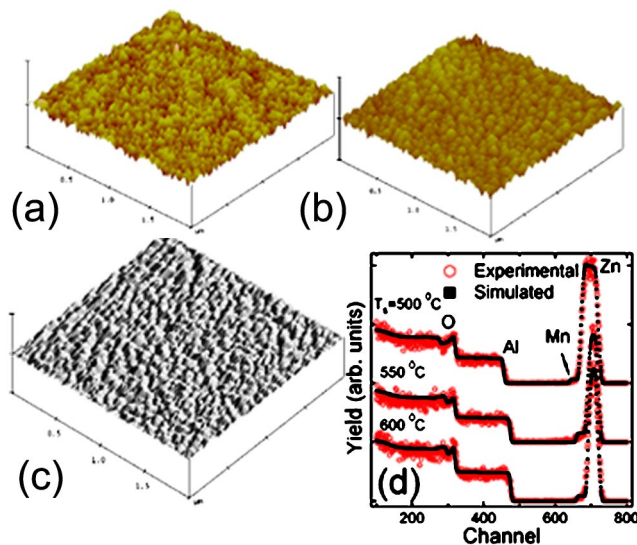


FIG. 2. (Color online) AFM pictures of (a) as-grown ZnMnO at  $T_s=500$  °C, (b) at  $T_s=600$  °C, and (c) at  $T_s=650$  °C. All scans are  $2\ \mu\text{m} \times 2\ \mu\text{m}$  in dimension. (d) RBS spectra of ZnMnO films grown at various temperatures. The simulated curves are also shown.

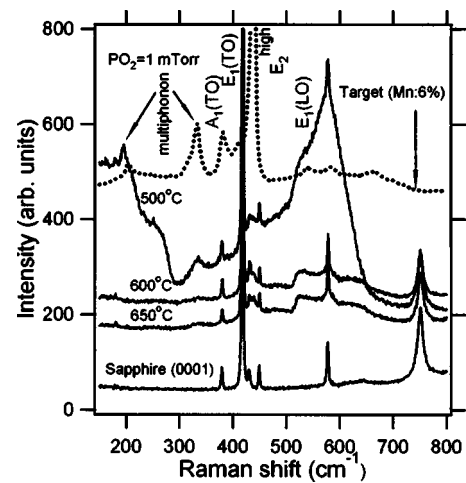


FIG. 3. Raman spectra of ZnMnO films grown at different substrate temperatures. The spectra for the substrate (sapphire) and the ZnMnO target are also shown.

markable improvement of the crystalline quality and surface morphology is very clear with the increasing  $T_s$ . The grain size dramatically increases with increasing  $T_s$ , resulting in high-quality epitaxial film grown at higher  $T_s$ . For example, the grain size increases from 50 nm to 65 nm with increasing  $T_s$  from 500 to 600 °C. The grains become very uniform and even coalesce in films grown at higher temperature, such as films grown at  $T_s=650$  °C. The surface roughness decreases from 3 nm to 2 nm (root-mean-square value) with increasing  $T_s$  from 500 to 600 °C.

The composition of the films was determined using 3 MeV  $He^{2+}$  RBS spectra. A typical result is shown in Fig. 2(d). The simulation of the RBS spectra was performed using GISA 3.9 program<sup>14</sup> assuming the composition to be  $Zn_{1-x}Mn_xO$ . The simulated results show that the film thickness is between 500 to 300 nm for films with  $T_s=500$  to 600 °C, respectively, and these are in good agreement with those obtained by stylus measurements. The random RBS spectra are very similar to simulated those based on the assumption of uniform Mn dispersion in ZnO. The RBS spectral lines are assigned to each elements present in the film. The simulated results from the RBS spectra give the composition of Zn:Mn:O=0.49:0.02:0.49 for  $T_s=500$  °C; and Mn=0.027 and 0.057 for  $T_s=550$  and 600 °C respectively. The increase in Mn concentration is believed to create isolated Mn clusters. A close inspection of the RBS spectra also shows that the peak due to Mn becomes more prominent with increasing  $T_s$ . The RBS spectra clearly illustrate that both crystalline quality and orientation improve with increasing  $T_s$ , which is consistent with the XRD results. In addition, RBS spectra also indicate that Mn diffuses into the sapphire substrates with increasing  $T_s$ .

Figure 3 shows the Raman spectra of ZnMnO films grown at various temperatures, sapphire substrate, and the target material. The most intense peak found at  $437\ \text{cm}^{-1}$  in film corresponds to the vibrational mode of  $E_2^{\text{high}}$ , and it is a typical Raman peak of ZnO bulk. The additional low intensity peaks observed in Fig. 3 are assigned to their respective modes. The modes at 203, 333, and 664, and above  $1000\ \text{cm}^{-1}$ , are due to the multiphonon scattering process. The  $E_2$  phonon mode centered on  $437\ \text{cm}^{-1}$  is obviously a good choice in order to understand the stress-induced phenomena in wurzite ZnO films. However, the  $E_2$  phonon fre-

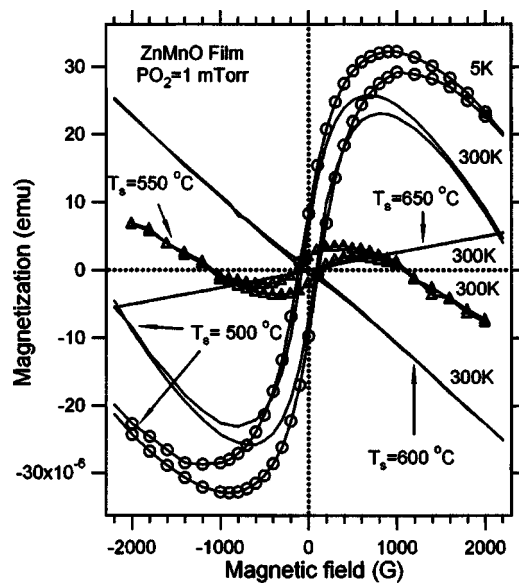


FIG. 4. Ferromagnetic hysteresis loops of ZnMnO films are shown for 5 and 300 K grown at  $T_s=500$  °C and for 300 K at  $T_s=550$ , 600, and 650 °C.

quency observed at  $437\text{ cm}^{-1}$  did not show any significant change in the Raman shift. In addition, we did not observe any extra peaks related to Mn, suggesting that Mn is incorporated into Zn. On the contrary, the RBS spectra show the presence of Mn clusters as shown in Fig. 2(d). However, the most remarkable feature in Raman spectra is the improvement in the crystalline quality with increasing  $T_s$ .

Figure 4 shows the magnetic field dependence of magnetization ( $MH$ ) curves at 5 and 300 K in ZnMnO film grown at  $T_s=500$  °C, exhibiting pronounced ferromagnetic behavior. The field at which the maximum in magnetization,  $H_m$  (low field to high field) is achieved decreases from 980 G at 5 K to 780 G at 300 K. However, the room-temperature ferromagnetic hysteresis shrinks with increasing  $T_s$ , illustrating a dominant competition between ferromagnetic-antiferromagnetic states.  $H_m$  decreases from 1000 G to about 400 G at 300 K with increase in  $T_s$  from 500 to 550 °C. It is noted that the background magnetic contribution due to sapphire substrate has not been corrected. This will further increase the  $H_m$  values. However, this will not affect the qualitative effects of  $T_s$  on magnetization because films with similar dimension were taken for the magnetic measurements. The magnetic measurements show an antiferromagnetic or paramagnetic behavior for films grown at higher  $T_s$  values, such as at 650 °C, as shown in Fig. 4, indicating the presence of Mn-related clusters, which may interact antiferromagnetically among each other. However, detail temperature dependent magnetization measurements are necessary to establish the nature of the actual magnetic state.

It was argued<sup>15</sup> that Mn–O–Mn clusters are favorable even at relatively lower doping level of Mn. Although  $\text{Mn}^{2+}$  ions can substitute  $\text{Zn}^{2+}$  sites homogeneously in the dilute limit,<sup>10</sup> the isolated state of  $\text{Mn}^{2+}$  is destroyed due to substitutional occupation of the nearest  $\text{Zn}^{2+}$  sites by other  $\text{Mn}^{2+}$  ions for increasing concentration of Mn. It was found that Mn atoms have a tendency to form clusters around oxygen on an epitaxial ZnMnO film.<sup>10</sup> However, the probability of

formation of clusters either in Mn–Mn or Mn–O–Mn form is low in a dilute limit where  $\text{Mn}^{2+}$  substitutes  $\text{Zn}^{2+}$  sites. Our magnetic experiments demonstrate that the substrate temperature plays a dominant role for determining the cluster density that determines the ferromagnetic behavior in ZnMnO films. On the other hand, a pronounced ferromagnetic behavior occurs at an optimum substrate temperature. This is in contrast to the recent experimental reports.<sup>1–12</sup> Although it remains challenging to utilize ferromagnetic Zn–MnO films for potential applications due to their relatively poor crystalline quality, a great deal of research is necessary for the optimization to obtain device-quality films. However, the unambiguous observation of ferromagnetism in this semiconductor is of intense scientific and technological interest.

In conclusion, we have demonstrated that ZnMnO films show remarkable ferromagnetic properties at room temperature when the films are grown at a substrate temperature of 500 °C and oxygen partial pressure of 1 mTorr. Although crystalline quality of the films is greatly improved with increasing substrate temperature, the ferromagnetic properties disappear. One of the main reasons of such disappearance of ferromagnetic behavior in ZnMnO may be related to formation of Mn-related clusters, which are favorably created at higher temperatures.

This work is supported by the National Aeronautics and Space Administration (NASA) and University Research Center (URC) cooperative agreement No. NCC-3-1035 and National Science Foundation (NSF) for Center for Research Excellence in Science and Technology (CREST) Grant No. HRD-9805059. Research at the University of Nebraska is supported by NSF-MRSEC, ONR, and CMRA. The authors are thankful to A. Wilkerson for experimental help.

<sup>1</sup>H. Ohno, *Science* **281**, 951 (1998); J. K. Furdyna, *J. Appl. Phys.* **64**, R29 (1988).

<sup>2</sup>B. Beschoten, P. A. Crowell, I. Malajovich, D. D. Awschalom, F. Matsukura, A. Shen, and H. Ohno, *Phys. Rev. Lett.* **83**, 3073 (1999).

<sup>3</sup>T. Dietl, H. Ohno, F. Matsukura, J. Cibert, and D. Ferrand, *Science* **287**, 1019 (2000).

<sup>4</sup>M. L. Reed, N. A. El-Masry, H. H. Stadelmaier, M. K. Ritums, M. J. Reed, C. A. Parker, J. C. Roberts, and S. M. Bedair, *Appl. Phys. Lett.* **79**, 3473 (2001).

<sup>5</sup>M. Linnarsson, E. Janzén, B. Monemar, M. Kleverman, and A. Thilderkvist, *Phys. Rev. B* **55**, 6938 (1997).

<sup>6</sup>M. E. Overberg, C. R. Abernathy, S. J. Pearton, N. A. Theodoropoulou, K. T. McCarthy, and F. Hebard, *Appl. Phys. Lett.* **79**, 1312 (2001).

<sup>7</sup>S. W. Jung, S.-J. An, G.-C. Yi, C. U. Jung, S. Lee, and S. Cho, *Appl. Phys. Lett.* **80**, 4561 (2002).

<sup>8</sup>V. A. L. Roy, A. B. Djuricic, H. Liu, X. X. Zhang, Y. H. Leung, M. H. Xie, J. Gao, H. F. Liu, and C. Surya, *Appl. Phys. Lett.* **84**, 756 (2004).

<sup>9</sup>Y. W. Heo, M. P. Ivill, K. Ip, D. P. Norton, S. J. Pearton, J. G. Kelly, R. Rairigh, A. F. Hebard, and T. Steiner, *Appl. Phys. Lett.* **84**, 2292 (2004).

<sup>10</sup>X. M. Cheng and C. L. Chien, *J. Appl. Phys.* **93**, 7876 (2003).

<sup>11</sup>T. Fukumura, Z. Jin, M. Kawasaki, T. Shono, T. Hasegawa, and H. Koimura, *Appl. Phys. Lett.* **78**, 958 (2001).

<sup>12</sup>S. W. Yoon, S.-B. Cho, S. C. We, S. Yoon, B. J. Shul, K. K. Song, and Y. J. Shin, *J. Appl. Phys.* **93**, 7879 (2003).

<sup>13</sup>P. Sharma, A. Gupta, K. V. Rao, F. J. Owens, R. Verma, R. Ahuja, J. M. O. Guillen, B. Johansson, and G. A. Gehring, *Nat. Mater.* **2**, 673 (2003).

<sup>14</sup>J. Saarilahti and E. Rauhala, *Nucl. Instrum. Methods Phys. Res. B* **64**, 734 (1992).

<sup>15</sup>Z. W. Jin, Y.-Z. Yoo, T. Sekiguchi, T. Chikyow, H. Ofuchi, H. Fujioka, M. Oshima, and H. Koimura, *Appl. Phys. Lett.* **83**, 39 (2003).